PAPER

Self-powered flexible piezoelectric nanogenerator made of poly (vinylidene fluoride)/Zirconium oxide nanocomposite

View the article online for updates and enhancements.

IOP ebooks™

Bringing you innovative digital publishing with leading voices to create your essential collection of books in STEM research.

Start exploring the collection - download the first chapter of every title for free.

Materials Research Express

PAPER

Self-powered flexible piezoelectric nanogenerator made of poly (vinylidene fluoride)/Zirconium oxide nanocomposite

Rahul Naik[1] and Somasekhara Rao T

Department of Mechanical Engineering, National Institute of Technology Karnataka, Surathkal, Karnataka, 575025, India
[1] Author to whom any correspondence should be addressed.

E-mail: rahulnaik94@gmail.com and ssrao@nitk.edu.in

Abstract

The electroactive β-phase is the most desirable due to its highest piezo-, pyro-, and ferroelectric properties in Poly (vinylidene fluoride) (PVDF). The β- phase can be nucleated by incorporation of nanoparticles into PVDF. The objective of this study is the preparation and characterization of the pristine PVDF film, and intensified dosages of the ZrO$_2$ modified composite PVDF films, further piezoelectric properties of nanocomposites films are evaluated. The nanocomposite films have been prepared by solution casting method with different loadings of ZrO$_2$. The prepared films are characterized by Scanning electron microscope (SEM), x-ray diffraction (X-RD) analysis, Fourier transform infrared spectra (FTIR), and Differential scanning calorimetry (DSC), to study surface morphology, β- phase content, crystallinity, and melting temperature. The experimental analysis shows that the β- phase percentage and melting temperature of the films increases with ZrO$_2$ loading, but the percentage of crystallinity decreases. Nanogenerators are fabricated by using the films, and piezoelectric performances of the nanogenerators are evaluated under various external stresses. The maximum voltage generated in the case of 10 wt% loading of ZrO is 670 mV for 100 g of load, which is approximately eight times higher than the voltage generated in the pristine- PVDF and 980 mV is generated while tapping by hand.

1. Introduction

Energy consumption is increasing day by day due to rapidly growing industrialization and population. Conventional sources (also called non-renewable sources) of energy, which mainly depends on fossil fuels, cause global warming, pollution of the environment, and energy crisis [1, 2]. Besides conventional sources of energy, there are non-conventional sources (also called renewable sources) of energy such as bioenergy, solar energy, wind energy, and tidal energy [3]. Recently, harvesting energy from ceramic-based piezoelectric materials has been actively investigated due to their piezoelectric, pyroelectric, and triboelectric properties. Energy harvested from these technologies can be used on low- powered and portable micro energy harvester to drive electronic devices and self- powered sensors to measure various physical/biological/chemical inputs in a precise manner in various environmental conditions. However, harvesting energy from ceramic-based piezoelectric materials have limitations related to device design, unstable output behaviour, and packaging issues etc To overcome these limitations, researchers are working on polymer-based materials to harvest energy. Piezoelectric energy harvested from polymer-based material can convert waste mechanical energy like human body movements (e.g. walking, running and finger movements), fluid motion, and machine vibrations into useful electrical energy [3–6]. A piezoelectric nanogenerator (PNG) is a device, which is capable of harvesting energy by converting external mechanical energy into electrical energy by using piezoelectric materials. Traditional PNGs, which are based on ceramic materials like lead zirconate titanate Pb(ZrTi)O$_3$, Barium titanate (BaTiO$_3$), and sodium niobate (NaNbO$_3$), have high piezoelectric coefficients [7–9]. However, these ceramic materials are toxic and hazardous to living beings. Also, these ceramic-based PNGs are brittle in nature and also difficult to mount on

complex surfaces [10, 11]. Therefore, researchers are working on PNGs, which are based on piezoelectric polymers such as Polyvinylidene fluoride (PVDF) and its copolymers as these are flexible and eco-friendly.

PVDF is known to be semi-crystalline and ferroelectric polymer. It has a simple repetitive unit of –(CH2–CF2). It has different crystalline phases such as α, β, γ, δ, and ε phases depending on their chain conformation. The α- phase has a monoclinic unit cell and consists of TGTG– conformation. The β and γ- phases have an orthorhombic unit cell with all trans (TTT) and TTTGTTTG conformations. The δ- phase is known to be polar and analogues of the α- phase, whereas the ε- phase is anti-polar and analogous to the δ- phase [12]. Among all the phases, the α- phase is most thermodynamically stable, but it does not show any piezoelectric property. It can be obtained directly from the melt. The β and γ- crystalline phases are known to be highly stable and exhibit piezoelectric property due to their polar crystalline electroactive nature. The β- phase exhibits more electroactive nature, when compared to the γ- phase, because all fluorine and hydrogen atoms are perpendicular to carbon backbone results in non-net zero dipole moment, which makes PVDF be a good piezo and ferroelectric polymer [13, 14]. Among all the phases of PVDF, the β- phase is the most important phase as it exhibits the highest electroactive nature, which makes it suitable for energy harvesting applications. There are different methods adopted to increase the β- phase in PVDF such as mechanical stretching at high temperature, uniaxial drawing, annealing, and high voltage poling [15–18]. Recent studies have focused on the addition of nanofillers such as metal nanoparticles, nanoclay, carbon nanotube, graphene, barium titanate, zinc oxide into PVDF to enhance the formation of the β- phase [19–24]. The addition of the nanofiller disrupts the molecular chain of the polymer, which leads to the enhancement of crystallinity and the β- phase producing the higher piezoelectric response. Ceramic based materials with high piezoelectric coefficients, such as lead zirconate titanate (PZT) have been added into the PVDF matrix to increase the overall piezoelectric response of the polymer nanocomposite. However, PZT is toxic and hazardous to living beings. It is also brittle, which limits the use of PZT as nanofiller into PVDF matrix [24]. However, it can be concluded, from the literature review, that the addition of different nanofillers into PVDF exhibits different percentages of the β-phase. This leads to variation in their piezoelectric responses. However, the β-phase alone is not responsible for the piezoelectric response. The interconnectivity of the neighboring dipoles and their arrangement are also involved in the piezoelectric response. So researchers are focusing their attention on piezopolymers over piezoceramic materials, due to their high flexibility, dimensional stability, high breakdown strength, thermal stability, and high piezoelectric response.

Herein, we report, for the first time, the enhancement of the β-phase by incorporation of zirconium oxide (ZrO$_2$) into PVDF polymer. The nanocomposite films, with various weights of ZrO$_2$ content (0, 1, 2, 3, 5 and 10 wt%), are prepared by using solution casting method. The detailed study on morphology, crystallinity, the β-phase content, and piezoelectric evaluation of the prepared nanocomposite films are investigated.

2. Experimental details

### 2.1. Materials used in the experimentation
The material used in this experiment is commercially available PVDF with molecular weight 180 000 g mol^{-1}, density 1.77 g cc^{-1}, melting point temperature 155 °C–160 °C. The material is purchased from M/s Arkema, France. Solvent N, N-dimethyl formamide (DMF) with 99% purity are purchased from Merck India Ltd The filler used is ZrO$_2$ purchased from sigma Aldrich India. All these materials are used without any purification.

2.2. Sample preparation method
To prepare PVDF/ZrO$_2$ solution, 1.2 g of PVDF powder is dissolved in 10 ml of DMF by magnetically stirring for 4 h at room temperature to obtain a homogeneous transparent solution. At the same time, the desired amount of ZrO$_2$ powder with different weight percentage (0, 1, 2, 3, 5 and 10 wt%) is dissolved separately in DMF by ultrasonication for 1 h to ensure fine dispersion of nanoparticles without forming agglomerates. In the next step, the dissolved nanoparticles are added to the PVDF solution and stirred for 8 h at 500 rpm. The homogeneous mixture solution is cast on a petri dish and kept in an oven for 3 h at 70 °C to get a flexible nanocomposite film. A schematic representation of fabrication set up of PVDF/ ZrO$_2$ nanocomposite film is shown in figure 1.

2.3. Characterisation of PVDF and PVDF/ZO$_2$ nanocomposite films
The prestine PVDF and PVDF/ZrO$_2$ nanocoposite films are characterisation by FE-SEM, FTIR, XRD and DSC, to check the surface morphology, % β- phase content, % crystallinity and melting temperature.
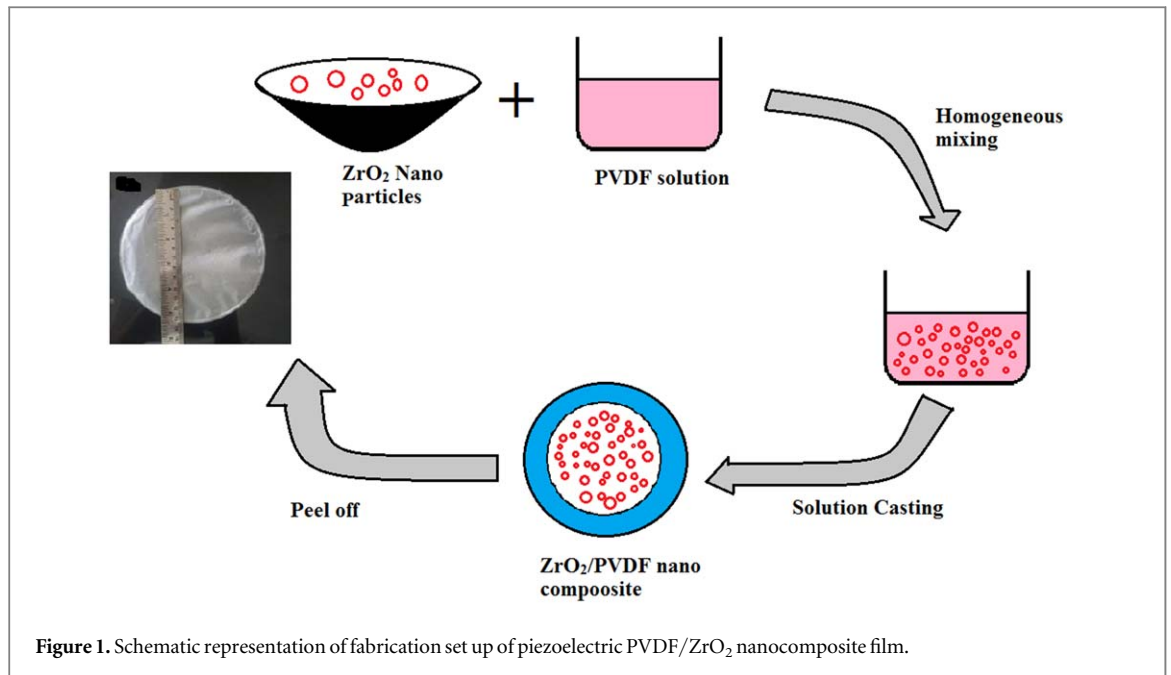
Figure 1. Schematic representation of fabrication set up of piezoelectric PVDF/ZrO$_2$ nanocomposite film.

2.3.1. Field emission scanning electron microscope (FE-SEM)

Surface morphologies of the nanocomposite films are analyzed using field emission scanning electron microscope (FE-SEM) with an accelerating voltage of 10 kV. A thin layer of gold is sputtered on the samples.

2.3.2. Fourier transform infrared spectroscopy (FTIR) analysis

FTIR analysis is carried out, using Jasco FTIR 4200 series spectrometer, to study the formation of the β- phases in PVDF nanocomposite films. The analysis is carried out in the range of 1600–650 cm^{-1} by KrBr pellet method at 1 cm^{-1} resolution. In pristine PVDF film and PVDF/ZrO$_2$ nanocomposite samples, the β- phase contents are calculated by using equation (1). Vibrational bands of the α and β-phases of the samples are compared. It is assumed that the absorption spectrum follows the Lambert-Beer law, which is given in equation (1).

$$F(\beta) = \frac{X_\beta}{X_\alpha + X_\beta} = \frac{A_\beta}{\left(\frac{K_\beta}{K_\alpha}\right)A_\alpha + A_\beta} \tag{1}$$

where, $X\alpha$ is the α- phase mass fraction, and $X\beta$ is the β- phase mass fraction. Aα and Aβ denote absorption intensity of the α-phase at 762 cm^{-1} and the β-phase at 840 cm^{-1} respectively, Kα and Kβ are absorption coefficients of the α and β- phases with values 6.1 $\times$ 10^4 cm^2 mol^{-1} and 7.7 $\times$ 10^4 cm^2 mol^{-1} respectively [24].

2.3.3. X-ray diffraction (XRD)

X-ray Diffraction is performed to study the degree of crystallinity and polymorphism of the samples. The diffraction patterns are recorded within the 2θ range of 10°–50° at a scanning speed of 1° min^{-1}. Degree of crystallinity (X_c) is calculated by using equation (2).

$$\%X_c = \frac{I_c}{I_a + I_c} \times 100 \tag{2}$$

where I_c and I_a are the corresponding integrated intensities peaks of crystalline and amorphous phases.

2.3.4. Differential scanning calorimetry (DSC)

DSC is used to study the phase transition, crystallinity, and melting temperature of the films. The tests are performed under nitrogen atmosphere flowing at a rate of 50 ml min^{-1} with a heating rate of 10 °C min^{-1} in the temperature range of 25 °C–225 °C. The percentage crystallinity of pristine PVDF and PVDF/ZrO$_2$ nanocomposites is calculated by using equation (3).

$$X_C = \frac{\Delta H_m}{H_m^\circ} \tag{3}$$

where, ΔH_m and $\Delta H^\circ m$ are apparent enthalpies and enthalpy of fusion respectively, and $\Delta H^\circ m$ value for 100% crystallinity per gram is 104.5 J g^{-1} [24].
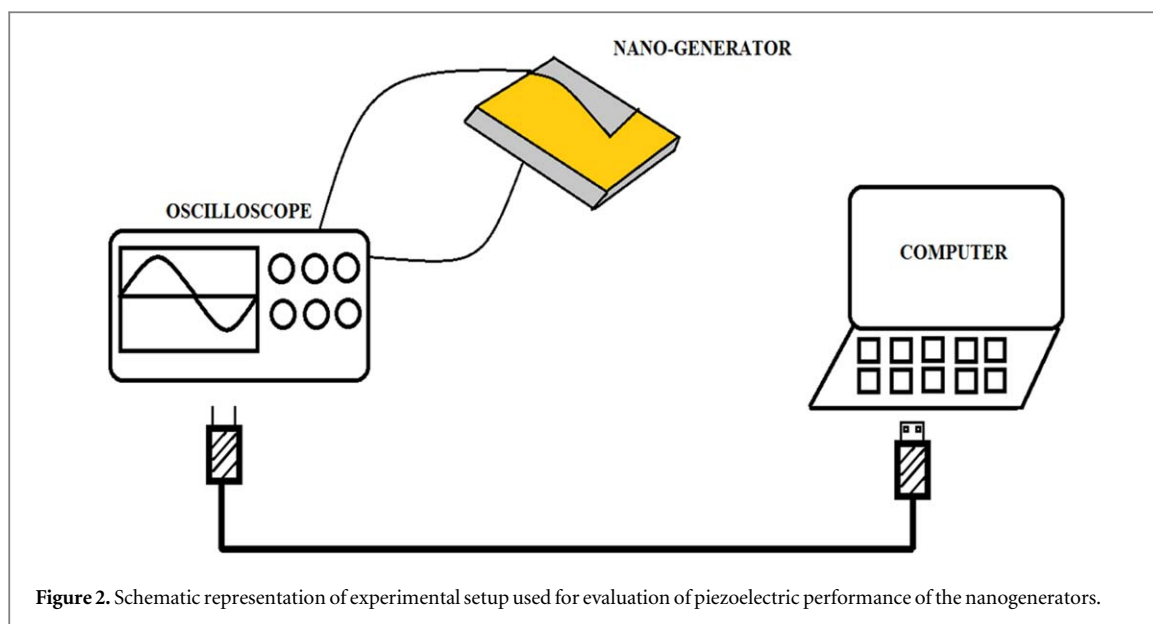
Figure 2. Schematic representation of experimental setup used for evaluation of piezoelectric performance of the nanogenerators.

2.3.5. Evaluation of Piezoelectric responses of the nanocomposite films

The schematic representation of the experimental setup used for the evaluation of the piezoelectric performance of nanogenerator is shown in figure 2. To measure the output voltage, the composite films are sandwiched between two copper electrodes (4.0 × 2.0 × 0.02 cm). The patch is covered with a flexible and transparent sheet of PVC. To avoid contact between the two electrodes, an insulating tape is pasted on the edges of the electrodes. The electrodes are then connected to the oscilloscope through single strand wires for measuring piezoelectric voltage output.

3. Results and discussion

3.1. FE-SEM analysis

Field emission scanning electron micrographs (FE-SEM) have been taken for the pristine PVDF, and PVDF with different loading of ZrO_2 (1, 2, 3, 5 and 10 wt%) are shown in figures 3(a)–(f). The pristine PVDF film shows a simple plain morphology as shown in figure 3(a). The fibril like spherulite structure is formed due to the random nucleation on the surface of the matrix which shows the α- phase of the pristine PVDF. For the PVDF/ZrO_2 nanocomposite, it shows a uniform distribution of the filler due to the functional group interaction between the polymer and the filler, as will be confirmed by other techniques later on.

The oxygen content in the functional groups that are present on the surface of zirconium could interact with the hydrogen bond of the PVDF polymer, which resulted in good dispersion of the filler inside the PVDF solution and also the surface charge of zirconium helped in the orientation of molecular chain due to ion-dipole interaction. SEM images indicate that nanoparticles are well dispersed into the PVDF solution up to 5% but as the nanoparticles are increased, a non-continuous structure has resulted from aggregation of the PVDF solution as we can see in 10% of zirconium content [25].

3.2. Fourier transformation infrared spectroscopy analysis

Fourier Transformation Infrared (FTIR) spectroscopy analysis for the pristine PVDF and PVDF nanocomposite films are shown in figure 4. The vibrational bands are seen due to the stretching of CF_2, C=C, and C–H bending vibrations. The FTIR spectrum shows dipole-dipole interaction between PVDF and ZrO_2. Vibrational bands are observed at 841 cm^{-1}, 1080 cm^{-1}, and 1400 cm^{-1} for the pristine PVDF and the PVDF/ZrO_2 nanocomposite films which indicate the formation of the β- phase. The 795 cm^{-1}, 878 cm^{-1}, and 1190 cm^{-1} vibrational bands predominantly indicate the α- phase of the PVDF [24, 26–28, 31]. All the composites indicate characteristic vibrational bands at 510 cm^{-1}, 615 cm^{-1} and 766 cm^{-1} are due to CF_2 bending, vibrational bands at 1190 cm^{-1} is due to CF_2 stretching, vibrational band at 841 cm^{-1} is due to CH_2 rocking, 1080 cm^{-1} and 1400 cm^{-1} are due to CH wagging [27, 29]. The β- phase in PVDF/ZrO nanocomposites are calculated by using equation (1).

The relative fractions for the β-phase using equation (1) are 18.7%, 25.2%, 33.8%, 57.1%, 62.1%, and 69.4% for the pristine PVDF, PVDF/1% ZrO, PVDF/2% ZrO, PVDF/3% ZrO , PVDF/5% ZrO , and PVDF/10% ZrO respectively. The results show that the β-phase fraction increased with zirconium nanoparticles increment up to 10%, after which there is decreased, which may be due to agglomeration of nanoparticles. The
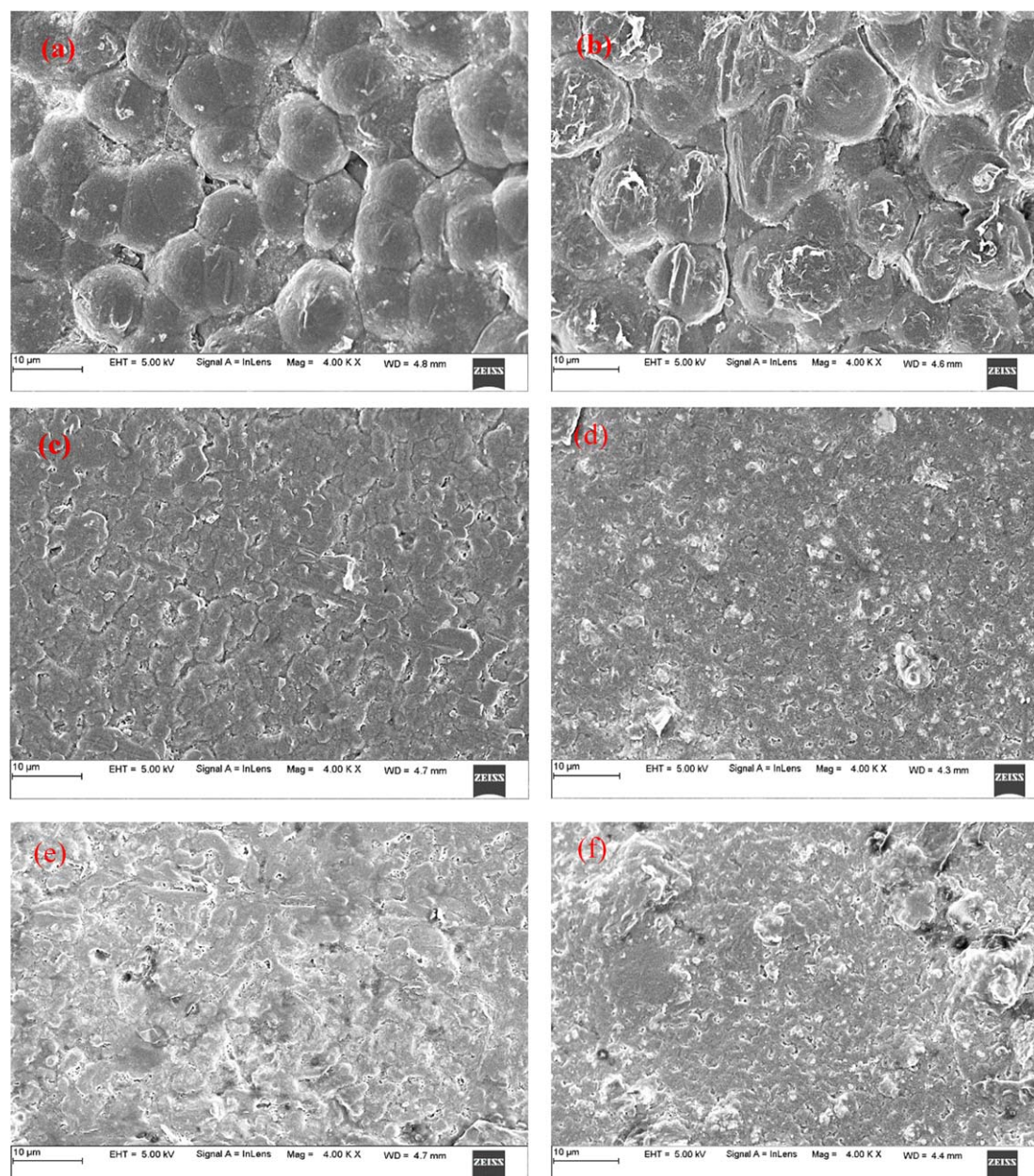
Figure 3. Field emission scanning electron (FE-SEM) micrographs of (a) the pristine PVDF (b)–(f) PVDF with 1, 2, 3,5 and 10 wt% ZrO_2 respectively.

increment in the β- phase (more chains are formed due to rearrangement of dipoles) is observed. Table 1. shows % β- phase content in the PVDF nanocomposites at increased loadings of zirconium.

3.3. X-ray diffraction studies

X-ray diffractographs (XRD) for the pristine PVDF and the PVDF nanocomposites are shown in figure 6. Peaks observed at 18.6°, 19.8° and 29.9° are characteristic of the α- phase, corresponding to (100), (020), and (021) planes of the PVDF nanocomposites respectively. The peak observed at 20.4° (110/220) for PVDF nanocomposites corresponds to the β- phase [27–29]. The new peaks observed at 27.5°, 29.7°, 36.5° for PVDF with 3%, 5% and 10% ZrO_2 nanocomposite samples are related to zirconium oxide [25, 30].

From figure 5, we can see the peak intensity corresponding to the α-phases decreases, while the intensity of the peak related to the β- phases increases as the zirconium loading increases. Degree of crystallinity (X) is calculated by using the equation (2). From the equation (2), the %crystallinity are 53.90%, 51.1%, 49.0%, 48.8%, 46.5% and 45.70% for the, pristine PVDF, PVDF/1%ZrO, PVDF/2%ZrO, PVDF/3%ZrO PVDF/5% ZrO and PVDF/10% ZrO respectively. Table2 shows % crystallinity of the PVDF nanocomposites at increased loadings of zirconium.
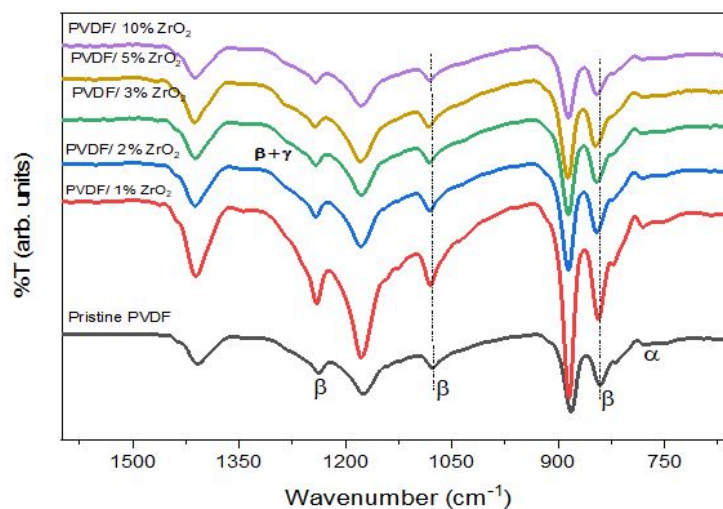
Figure 4. FTIR spectra of the pristine-PVDF and the PVDF nanocomposites at increased loadings of ZrO_2 nanoparticles.
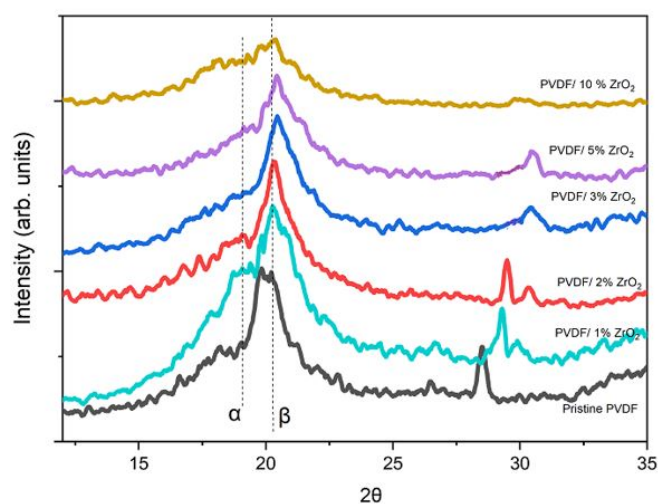

Figure 5. XRD patterns of the pristine- PVDF and the PVDF nano-composites at increased loadings of ZrO_2 nanoparticles.

Table 1. % β- phase content of PVDF with increased concentration of Zirconium.

Sample	β- phase (%)
pristine PVDF	18.7
PVDF/1% ZrO_2	25.2
PVDF/2% ZrO_2	33.8
PVDF/3% ZrO_2	57.1
PVDF/5% ZrO_2	62.1
PVDF/10% ZrO_2	69.4

3.4. Differential scanning calorimetry analysis

Differential Scaqwnning Calorimetry (DSC) curves of the pristine PVDF and the PVDF composites with increased loading of zirconium nanoparticles are shown in figure 7. For the pristine PVDF, the melting point is 177.2 °C. For nanocomposites, the melting point of the PVDF has shifted to higher values as zirconium nanoparticles increased. The increment in melting point confirmed the rearrangement of the PVDF chain

Figure 6. DSC curves of the pristine PVDF and the PVDF nanocomposites at increased loadings of ZrO$_2$.

Figure 7. Piezoelectric responses of the pristine PVDF and the PVDF composites at increased loadings of ZrO$_2$.
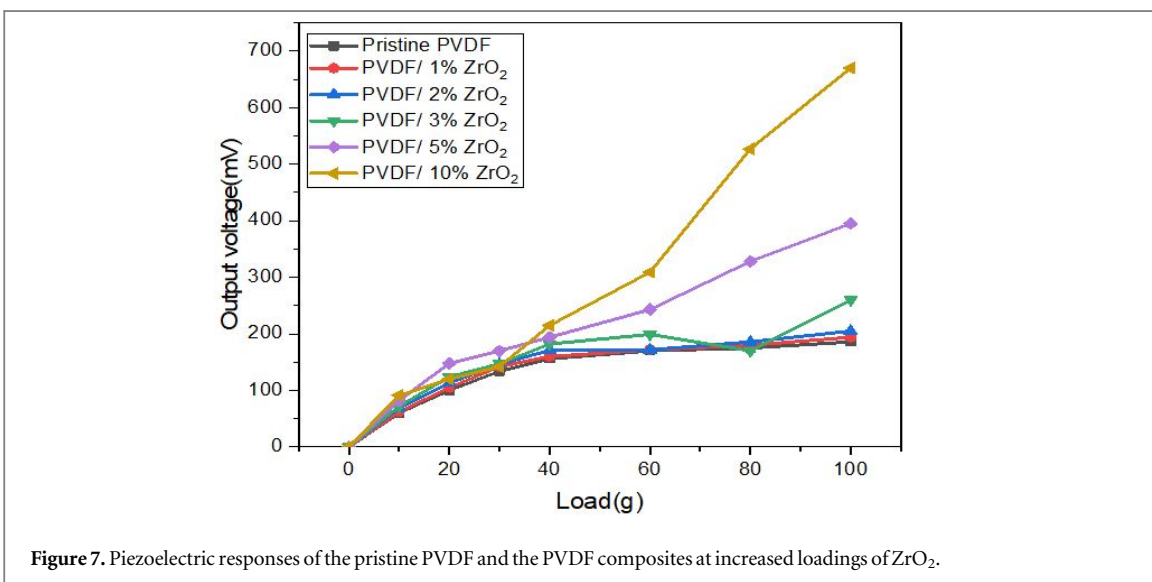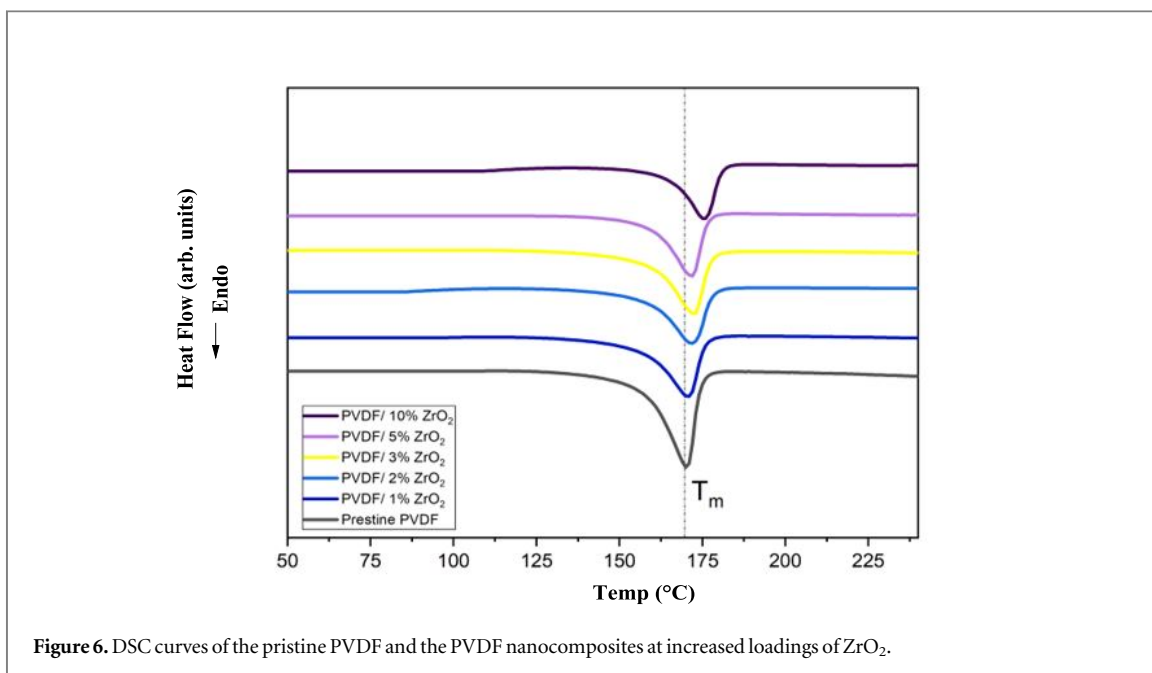
Table 2. % Crystallinity of the PVDF nanocomposites at increased loadings of zirconium.

Samples	2Ө	% Crystallinity
pristine PVDF	20.38	53.90
PVDF/1% ZrO$_2$	20.40	51.10
PVDF/2% ZrO$_2$	20.40	49.00
PVDF/3% ZrO$_2$	20.45	49.80
PVDF/5% ZrO$_2$	20.45	46.50
PVDF/10% ZrO$_2$	20.50	45.70

conformation due to the addition of zirconium. The % crystallinity of the pristine PVDF and the PVDF nanocomposites are calculated using equation (3).

From equation (3), the %crystallinity of the pristine PVDF is determined to be 53.1% and 50.4%, 48.5%, 48.2%, 45.6%, 44.9% for PVDF/1%ZrO, PVDF/2%ZrO, PVDF/3%ZrO, PVDF/5%ZrO and PVDF/10% ZrO$_2$ respectively and tabullated in table 3. The % X_c of the PVDF nanocomposites decreases with increase

Table 3. Melting temperature and degree of crystallinity of the PVDF nanocomposites.

Samples	Melting temperature (°C)	% Crystallinity
pristine PVDF	170.2	53.1
PVDF/1% ZrO_2	171.4	50.4
PVDF/2% ZrO_2	172.5	48.5
PVDF/3% ZrO_2	172.5	48.2
PVDF/5% ZrO_2	174.0	45.6
PVDF/10% ZrO_2	174.7	44.9

in loadings of zirconium nanoparticles up to 5%, later increased. From all the above results, it can be concluded that the fillers are dispersed uniformly in the matrix upto 10% ZrO, at higher loading (10%), ZrO agglomerates results an increase in crystallinity. The fillers interrupt packaging of the polymer chain, which has lead to a decrease in the crystallinity.

As we discussed earlier, PVDF is a polymer with linear hydrocarbon consisting of repeated units of CH_2 CF_2 monomers. Depending on the chair rearrangement of fluoride and hydrogen atoms, PVDF present in α, β, γ, δ, and ε phases. The α-phase has $TGTG^-$ conformation. The β- phase all trans (TTT) and TTTGTTTG conformations. Among all, the β- phase exhibits more electroactive nature, because all fluorine and hydrogen atoms are perpendicular to carbon backbone. This promotes non-net zero dipole moment, which makes PVDF to be a good piezo and ferroelectric polymer. When we add ZrO_2 nanoparticles into the PVDF matrix, the surface charges of ZrO_2 interact with CH_2CF_2 monomers of PVDF polymer. Which means positively charged atoms interacts with CF_2 monomer and negatively charged atoms interacts with CH_2 monomer. This interaction prompts the arrangement of the polymer chain of PVDF by the addition of ZrO_2, results in the formation of all trans conformations. Which implies that there is the development of β-phase in PVDF/ ZrO_2 polymer nanocomposite films. Which is confirmed in the FTIR results. For PVDF/10% ZrO_2 nanocomposite film, the % β- phase content is 69.4%, but for pristine PVDF film, it is 18.7%.

3.5. Piezoelectric performance of nanogenerators

The piezoelectric performance and energy harvesting capability are evaluated under various modes. When mechanical pressure (stress) is applied on the surface of a nanogenerator, the strain is generated, which produces deformation in the crystal structure (shifting of positively charged hydrogen atoms and negatively charged fluoride atoms). This deformation leads to the generation of the piezoelectric effect. This piezoelectric potential creates a charge potential on the electrodes. The piezoelectric voltage is observed due to the flow of electrons towards the external circuit because of the difference in piezoelectric potential.

The piezoelectric performances of the pristine PVDF nanogenerator and the PVDF nanocomposite nanogenerators with increased loading of zirconium under varying static loads are evaluated. A maximum voltage output of 160 mV is observed in the case of pristine PVDF based nanogenerator, while it is 670 mV in case of the PVDF/10% ZrO based nanogenerator, at 100 g of static load. The piezoelectric performance is increased as shown in

The performances of the nanogenerators are evaluated under human locomotion (tapping on the nanogenerators). The highest voltage of 980mV is observed incase of the PVDF/10% ZrO based nanogenerator. The improved piezoelectric performance of the nanogenerators due to addition of ZrO could play a vital role in the development of flexible, cheap self -controlled electronic devices.

4. Conclusions

The flexible PVDF/ZrO_2 nanocomposite film based nanogenerators can be used for energy harvesting applications. Addition of ZrO_2 into the PVDF polymer enhances the β-phase content due to the interaction between the surface charge of zirconium and $–CH_2–CF_2–$ dipoles of the PVDF nanocomposites. The thermal properties of the nanogenerators have improved, while the crystallinity has decreased with the increase of ZrO content up to 10wt%ZrO. The piezoelectric output voltage for the pristine PVDF nanogenerator is 160mV. However, as the filler content is increased, the piezoelectric performance also has increased and shown a maximum output voltage of 670mV at 10wt% ZrO content, which is nearly four times higher than pristine PVDF based nanogenerator. The flexible nanogenerators developed in this work has the potential to be used as flexible nanosensors and the self- powered devices.

ORCID iDs

Rahul Naik ⬤ https://orcid.org/0000-0002-7389-3933

References

[1] Mane P, Xie J, Leang K K and Mossi K 2011 Cyclic energy harvesting from pyroelectric materials *IEEE Trans. Ultrason. Ferroelectr. Freq. Control* **58** 10–7

[2] Kar E, Bose N, Dutta B, Banerjee S, Mukherjee N and Mukherjee S 2019 2D SnO$_2$ nanosheet/PVDF composite based flexible, self-cleaning piezoelectric energy harvester *Energy Convers. Manage.* **184** 600–8

[3] Wang Z L and Wu W 2012 Nanotechnology-enabled energy harvesting for self-powered micro-/nanosystems *Angew. Chem. Int. Ed.* **51** 11700–21

[4] Kiti Kwuimy C A, Litak G, Borowiec M and Nataraj C 2012 Performance of a piezoelectric energy harvester driven by air flow *Appl. Phys. Lett.* **100** 024103

[5] Dias J A C, De Marqui C Jr and Erturk A 2013 Hybrid piezoelectric-inductive flow energy harvesting and dimensionless electroaeroelastic analysis for scaling *Appl. Phys. Lett.* **102** 044101

[6] Beeby S P, Tudor M J and White N M 2006 Energy harvesting vibration sources for microsystems applications *Meas. Sci. Technol.* **17** R175

[7] Xu S, Hansen B J and Wang Z L 2010 Piezoelectric-nanowire-enabled power source for driving wireless microelectronics *Nat. Commun.* 93

[8] Zhou B, Li R, Cai J, Xu J, Zhao Z and Pei J 2018 Grain size effect on electric properties of novel BaTiO3/PVDF composite piezoelectric ceramics *Mater. Res. Express* **5** 095510

[9] Anand A and Bhatnagar M C 2018 Effect of sodium niobate (NaNbO$_3$) nanorods on β-phase enhancement in polyvinylidene fluoride (PVDF) polymer *Mater. Res. Express* **6** 055011

[10] Rubio-Marcos F, López-Juárez R, Rojas-Hernandez R E, del Campo A, Razo-Pérez N and Fernandez J F 2015 Lead-free piezoceramics: revealing the role of the rhombohedral–tetragonal phase coexistence in enhancement of the piezoelectric properties *ACS Applied Materials & Interfaces* **7** 23080–8

[11] Arlt K and Wegener M 2010 Piezoelectric PZT/PVDF-copolymer 0-3 composites: aspects on film preparation and electrical poling *IEEE Trans. Dielectr. Electr. Insul.* **17** 1178–84

[12] Martins P, Lopes A C and Lanceros-Mendez S 2014 Electroactive phases of poly (vinylidene fluoride): determination, processing and applications *Prog. Polym. Sci.* **39** 683–706

[13] Liu Z H, Pan C T, Yen C K, Lin L W, Huang J C and Ke C A 2015 Crystallization and mechanical behavior of the ferroelectric polymer nonwoven fiber fabrics for highly durable wearable sensor applications *Appl. Surf. Sci.* **346** 291–301

[14] Lee J S, Shin K Y, Kim C and Jang J 2013 Enhanced frequency response of a highly transparent PVDF–graphene based thin film acoustic actuator *Chem. Commun.* **49** 11047–9

[15] Sencadas V, Moreira M V, Lanceros-Méndez S, Pouzada A S and GregórioFilho R 2006 α- to β Transformation on PVDF films obtained by uniaxial stretch *Mater. Sci. Forum* **514** 872–6 Trans Tech Publications

[16] Yee W A, Kotaki M, Liu Y and Lu X 2007 Morphology, polymorphism behavior and molecular orientation of electrospun poly (vinylidene fluoride) fibers *Polymer* **48** 512–21

[17] Hu Y C, Hsu W L, Wang Y T, Ho C T and Chang P Z 2014 Enhance the pyroelectricity of polyvinylidene fluoride by graphene-oxide doping *Sensors* **14** 6877–90

[18] Kaura T, Nath R and Perlman M M 1991 Simultaneous stretching and corona poling of PVDF films *J. Phys. D: Appl. Phys.* **24** 1848

[19] Rahman W, Ghosh S K, Middya T R and Mandal D 2017 Highly durable piezo-electric energy harvester by a super toughened and flexible nanocomposite: effect of laponitenano-clay in poly (vinylidene fluoride) *Mater. Res. Express* **4** 095305

[20] Kim G H, Hong S M and Seo Y 2009 Piezoelectric properties of poly (vinylidene fluoride) and carbon nanotube blends: β-phase development *Phys. Chem. Chem. Phys.* **11** 10506–12

[21] Hu Y C, Hsu W L, Wang Y T, Ho C T and Chang P Z 2014 Enhance the pyroelectricity of polyvinylidene fluoride by graphene-oxid doping *Sensors* **14** 6877–90

[22] Olmos D, González-Gaitano G, Kholkin A L and González-Benito J 2013 Flexible PVDF-BaTiO$_3$ nanocomposites as potential materials for pressure sensors *Ferroelectrics* **447** 9–18

[23] Chavan S, Gumtapure V and Perumal D A 2019 Characterization of linear low-density polyethylene with graphene as thermal energy storage material *Mater. Res. Express* **6** 065511

[24] Bafqi M S S, Bagherzadeh R and Latifi M 2015 Fabrication of composite PVDF-ZnO nanofiber mats by electrospinning for energy scavenging application with enhanced efficiency *J. Polym. Res.* **22** 130

[25] Aravindan V, Vickraman P and Kumar T P 2007 ZrO$_2$ nanofiller incorporated PVC/PVdF blend-based composite polymer electrolytes (CPE) complexed with LiBOB *J. Membr. Sci.* **305** 146–51

[26] Li J, Zhao C, Xia K, Liu X, Li D and Han J 2019 Enhanced piezoelectric output of the PVDF-TrFE/ZnO flexible piezoelectric nanogenerator by surface modification *Appl. Surf. Sci.* **463** 626–34

[27] Salimi A and Yousefi A A 2003 Analysis method: FTIR studies of β-phase crystal formation in stretched PVDF films *Polym. Test.* **22** 699–704

[28] Sinha T K, Ghosh S K, Maiti R, Jana S, Adhikari B, Mandal D and Ray S K 2016 Graphene-silver-induced self-polarized PVDF-based flexible plasmonic nanogenerator toward the realization for new class of self-powered optical sensor *ACS Applied Materials & Interfaces* **8** 14986–93

[29] Nunes-Pereira J, Sencadas V, Correia V, Cardoso V F, Han W, Rocha J G and Lanceros-Méndez S 2015 Energy harvesting performance of BaTiO$_3$/poly (vinylidene fluoride–trifluoroethylene) spin coated nanocomposites *Composites Part B: Engineering* **72** 130–6

[30] Solarajan A K, Murugadoss V and Angaiah S 2017 Dimensional stability and electrochemical behaviour of ZrO$_2$ incorporated electrospun PVdF-HFP based nanocomposite polymer membrane electrolyte for Li-ion capacitors *Sci. Rep.* **7** 45390

[31] Lanceros-Mendez S, Mano J F, Costa A M and Schmidt V H 2001 FTIR and DSC studies of mechanically deformed β-PVDF films *Journal of Macromolecular Science, Part B* **40** 517–27